SUSTAINED LOAD CRACK GROWTH IN AN ALUMINIUM-SILICON BRONZE ALLOY

R.D. Scheffel*, M.A. Phoplonker, J. Byrne**, R.L. Jones*** and P. Barnes****

Crack growth under sustained constant load has been studied for an aluminium-silicon bronze alloy in room temperature air using pre-cracked bend specimens. The cracks were found to bifurcate and advance macroscopically in the directions of maximum shear stress in the plastic zone of the fatigue pre-crack. On the microscale the sustained load cracking was intergranular whilst final fracture was by a normal ductile mechanism. The incubation period for the onset of crack growth and time to failure were found to be strongly stress dependent and an influence of moisture in the environment was also indicated.

INTRODUCTION

Copper-aluminium alloys have a high tensile strength and good corrosion resistance in seawater. These properties are of paramount importance in marine applications e.g. fasteners, propellers. However, failures have occurred in fasteners under sustained and cyclic loading in air. A full understanding of the failure mechanism has not yet been fully established. Some early investigations have been conducted to study the influence of chemical composition on mechanical properties and stress corrosion resistance in different environments (1-6). Jones and Murphy (4) found that in air the UTS and the % elongation decreased drastically with decreasing strain rate. At a strain rate of 1 x 10^{-3} sec^{-1} the fracture was transgranular showing ductile dimpling but at a strain rate of 1 x 10^{-6} sec^{-1} indications of intergranular cracking were evident. At this lower strain rate the fractures showed typical characteristics of stress corrosion cracking (SCC).

* Universitat Siegen, D5900, Siegen, FRG
** Portsmouth Polytechnic, Portsmouth, U.K.
*** ARE Holton Heath, U.K.
**** ARE Dockyard Laboratory, Portsmouth, U.K.

MATERIAL DETAILS AND EXPERIMENTAL PROCEDURE

An aluminium-silicon bronze alloy (ASB) was studied. Three point bend specimens were machined longitudinally from 36 mm hexagonal bars. The bars had been hot extruded and drawn to size at 860/870 °C and then stress relieved/annealed at 350/400 °C for thirty minutes. The nominal dimensions of the three point bend specimens are shown in Fig. 1. Typical chemical composition and mechanical properties are given in Table 1.

TABLE 1 - Chemical Composition (weight %)

Al	Si	Fe	Ni	Mn	Sn
6.47	2.29	0.48	0.02	0.18	< 0.01
Pb	**Zn**	**Mg**	**Cu**		
< 0.01	< 0.02	0.18	remainder		

Mechanical Properties at Room Temperature

UTS	Proofstress	Elongation	Vickers-hardness	Modulus of Elasticity
MPa	0.2%, MPa	%		GPa
645	394	36	212	110

Fatigue precracking was carried out using an electro-magnetic resonance machine to obtain an a/W ratio of about 0.6 at a stress ratio of 0.1 and a final stress intensity range, ΔK, of 25 MPa$\sqrt{m}$.

The sustained load tests were performed in three point and cantilever bend rigs and crack growth was monitored using the direct current potential drop (DCPD) technique. Additionally the load line displacement was monitored using a linear voltage displacement transducer (LVDT).

The specimens were prepared for microstructural investigations by sawing off about 2 cm from each side of the notch; this section was then subsequently slit in half across the thickness. One half was examined using light microscopy whilst the second half was broken open for fractographic analysis on a scanning electron microscope (SEM).

RESULTS

The DCPD and LVDT methods were sufficiently sensitive to indicate crack advance under sustained load. The results in Fig. 1 show that an incubation period exists before crack advance under sustained load starts. This period and the time to failure depend on the load and environmental conditions. The lower the load controlling the initial value of stress intensity factor, Ki, the longer is the incubation period and the time to failure. A change of environment from laboratory air to a dry nitrogen atmosphere has the same effect, Fig. 2. However, a quantitative evaluation of these data to obtain crack propagation curves is not yet possible since the sustained load crack is bifurcated (Fig. 3).

The microstructure of this alloy includes both primary α grains and α transformed from β, with dispersed intermetallic (k) precipitates. In Fig. 4 the dark film on the grain boundaries suggests the possible presence of k-phase. Fig. 5 shows some details of the sustained load crack. It starts from one corner of the blunted fatigue crack tip and consists of two branches (Fig. 5a). They are of nearly equal lengths and the direction of each branch is approximately 70 degrees from the uncracked ligament. Fig. 5b shows a crack tip. It can be clearly seen that cracking occurs along the grain boundaries.

Fig. 6a shows the fracture surface under the SEM. Three types of cracking can be distinguished. These are the fatigue precrack, sustained load cracking and the final fracture. At higher magnification these fracture modes can be identified clearly as shown in Figs. 6b-d. The fatigue mode (Fig. 6b) is transgranular with some secondary cracking and some striated areas can be found. The final fracture (Fig. 6d) occurs by transgranular micro-void coalescence. At the surface of the specimen no sustained load cracking occurred whereas in the centre the extension was found to be several millimetres. The fracture surface (Fig. 6c) seems to indicate a brittle type of fracture along the grain boundaries. However, examining the fracture surface at higher magnification shows that a considerable amount of plastic deformation has been involved during fracturing since most of the grain surfaces are covered with slip lines (Figs. 7a,b).

DISCUSSION

Examining the micrographs initially (Figs. 5 and 6c), it was thought that two possible types of mechanism could be responsible for the sustained load fracturing. Namely, hydrogen embrittlement or stress corrosion cracking. In order to decide which of the two mechanisms were dominant some additional tests were conducted to investigate the possible influence of hydrogen. Two identical fatigue pre-cracked three point bend specimens were tested as

described earlier after each one had been treated differently prior to testing; one was heated in a vacuum furnace at 150/180 °C for 24 hours to reduce the amount of hydrogen present, whereas the other one was charged for half an hour as a cathode in an electrolytic cell with a solution of 3% Na Cl and at a current of 180 mA to enrich it with hydrogen.

The times taken to fracture both specimens to the same extent, were within the range of scatter found earlier. No major differences could be detected under the SEM to suggest that the influence of hydrogen is a significant factor.

The investigation has revealed that for this sustained load type of fracture, high stresses but a low strain rate are essential and there is an influence of moisture from the environment. The 70 degree angles found in the light microscopic investigation (Fig. 5a) are the angles under which the largest extension of the plastic zone in plane strain is to be expected according to a finite element analysis by Levy et al (7). The highest shear stresses in planes through the fatigue pre-crack tip occur in this direction as continuum fracture mechanics shows (Broek (8)). Link and Munz (9,10) found the same angle between a fatigue pre-crack and bifurcated stress corrosion cracks in bend specimens of the titanium alloy Ti Al6 V4 after tests in 3.5% Na Cl solution.

The appearance of high local strain can be detected from the higher magnification SEM results, Fig. 7. These micrographs show that the fractured grain boundaries are covered with a significant number of slip lines. The slip line spacing is about 0.5 μm. Straight slip lines are normally associated with face centred cubic metals of low stacking fault energies (11). A low stacking fault energy leads to coarse planar slip and pile-ups of dislocations at grain boundaries. Since the tip of a pile-up is associated with a high local stress, fracturing along grain boundaries could be significantly favoured by a film of a third phase (e.g. k-phase in this alloy) reducing the fracture toughness of the grain boundary. Furthermore these high strain regions allow the diffusion of some of the elements of the environment to the head of the pile-up and assist the process of fracture. Intergranular fracture in different copper aluminium alloys was also found by Higo et al (12) in fatigue crack propagation tests near the threshold. Under near-threshold conditions the present alloy shows the same effect, as shown by Phoplonker et al (13). Higo et al argue that intergranular cracking could possibly be associated with preferential oxidation along grain boundaries at the crack tip.

CONCLUSIONS

(i) Sustained load cracking in this aluminium-silicon bronze alloy occurs in room temperature air in an intergranular mode.

(ii) The incubation period for the onset of cracking and time to failure are strongly stress dependent.

(iii) The extended incubation period and time to failure in dry nitrogen indicates an influence of moisture on the crack growth mechanism.

ACKNOWLEDGEMENT

This work has been carried out with the support of Procurement Executive, Ministry of Defence.

REFERENCES

(1) Blackwood, A.W. and Stoloff, N.S., Trans. of the ASM, 1969, Vol. 62, pp.677-689.

(2) Ahmad, Z., Ghafelehbashi, M. and Nategh, S., Anti-Corrosion, August 1974, pp.13-16.

(3) Jones, R.L. and Murphy, S., Metals Technology, 1981, Vol. 6, pp.245-249.

(4) Jones, R.L. and Murphy, S., Br. Corros. J., 1983, Vol. 18, No. 3, pp.123-131.

(5) Cairns, W.J., Goodwin, R.J. and Stephens, D.M., Inst. of Metal Monograph, 1970, No. 34, pp.244-248.

(6) Parkins, R.N. and Suzuki, Y., Corrosion Science, 1983, Vol. 23, No. 6, pp.577-599.

(7) Levy, N., Marcal, P.V., Ostergren, W.J. and Rice, J.R., Int. Journ. Fracture Mech., 1971, Vol. 7, pp.143.

(8) Broek, D. Elementary Engineering Fracture Mechanics, Noordhoff International Publishing, Leyden, 1974, p.88.

(9) Link, F. and Munz, D., Corrosion Science, Vol. 13, 1973, pp.809-811.

(10) Link, F., Einfluss der Belastungsgeschwindigkeit auf das unterkritische Risswachstum mit und ohne Korrosionseinwirkung bei Ti Al6 V4 und Al Zn Mg Cul,5, DLr-FB 74-14, DFVLR, 1974.

(11) Avery, D.H. and Backofen, W.A., Acta Metallurgica, Vol. 11, 1963, pp.653-661.

(12) Higo, Y., Pickard, A.C. and Knott, J.F., Metal Science, 1981, pp. 233-240.

(13) Phoplonker, M.A., Scheffel, R., Byrne, J., Duggan, T.V. and Barnes, P., Submitted for presentation at the conference 'Fatigue of Engineering Materials and Structures' (FEMS), 15-19th Sept. 1986, Sheffield, U.K.

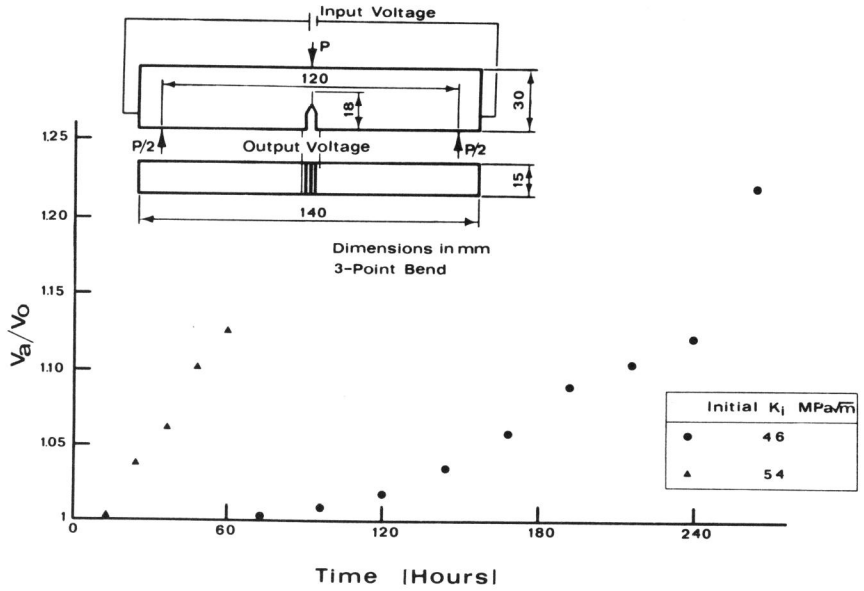

Fig. 1. Variation of DCPD Measurements Against Time in Room Temperature Air

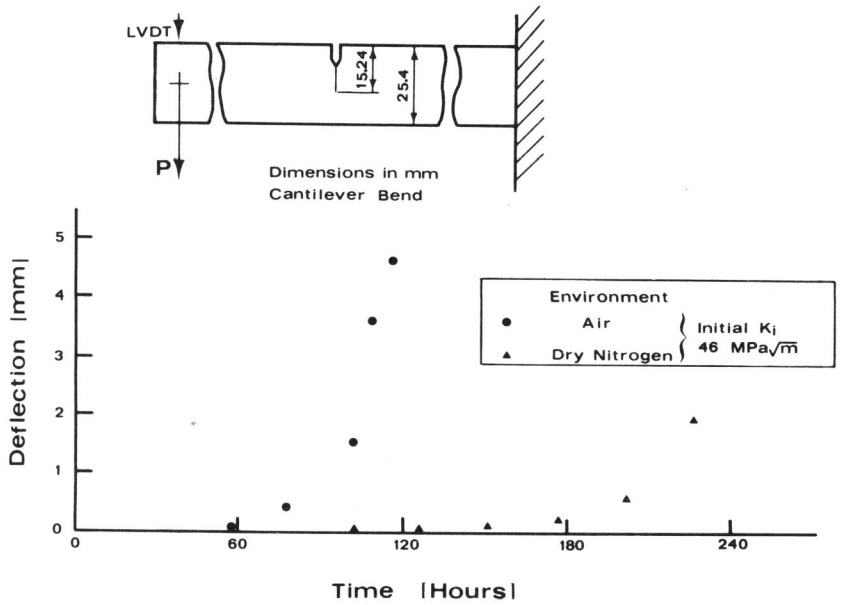

Fig. 2. Variation of LVDT Measurements Against Time in Room Temperature Air and Dry Nitrogen Environment

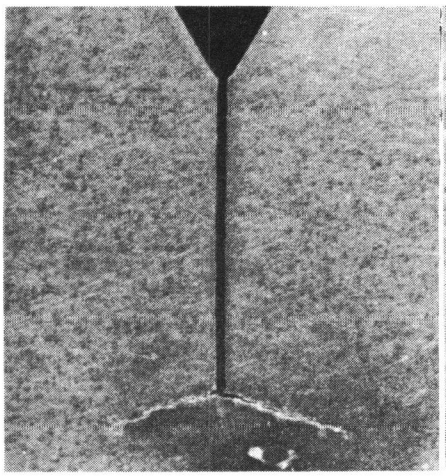

Fig. 3. Sustained Load Crack Branching: Mid-Thickness (X20)

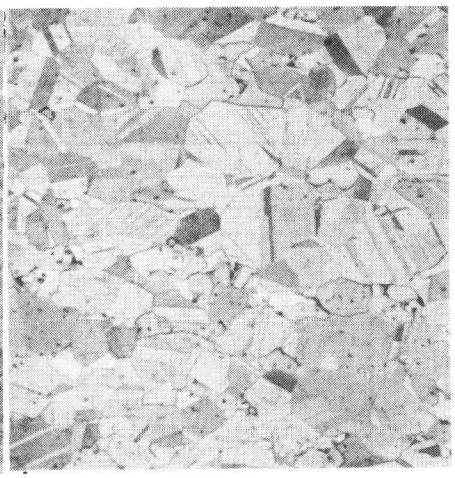

Fig. 4. Microstructure of ASB (X400)

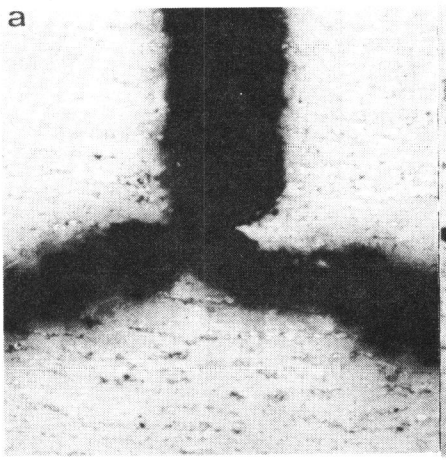

Start of sustained load cracking from end of fatigue crack (X40)

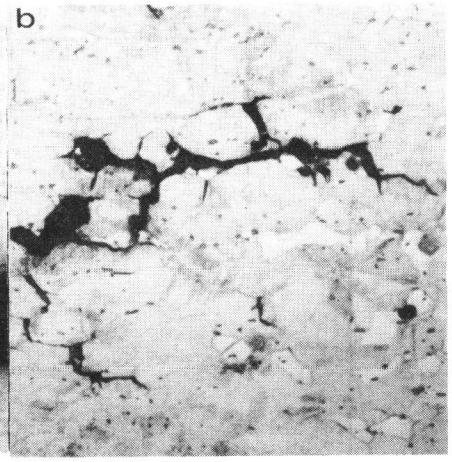

Crack tip-right hand side (X200)

Fig. 5. Microstructure Showing Sustained Load Crack Growth (Fig. 3, 4 and 5 all Alcoholic Ferric Chloride Etched)

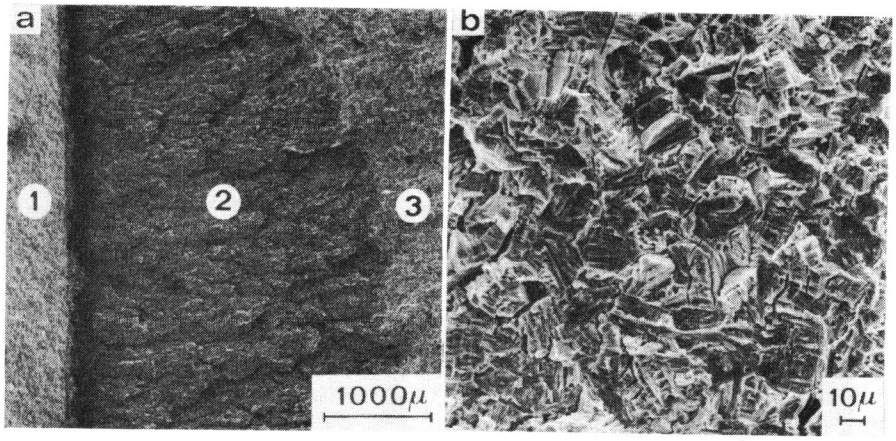

(1) Fatigue: transgranular
(2) Sustained load: intergranular
(3) Final Fracture: microvoid coalescence

Fatigue: transgranular

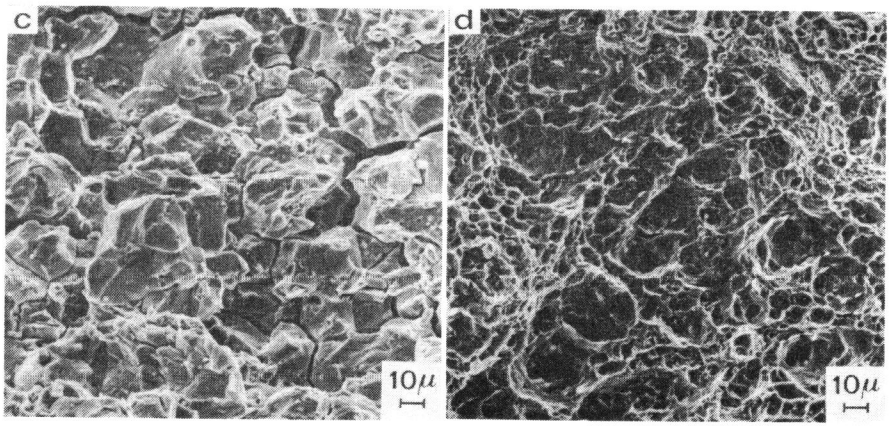

Sustained load: intergranular

Final fracture: microvoid coalescence

Fig. 6 SEM Fractographs Showing the Three Modes of Failure

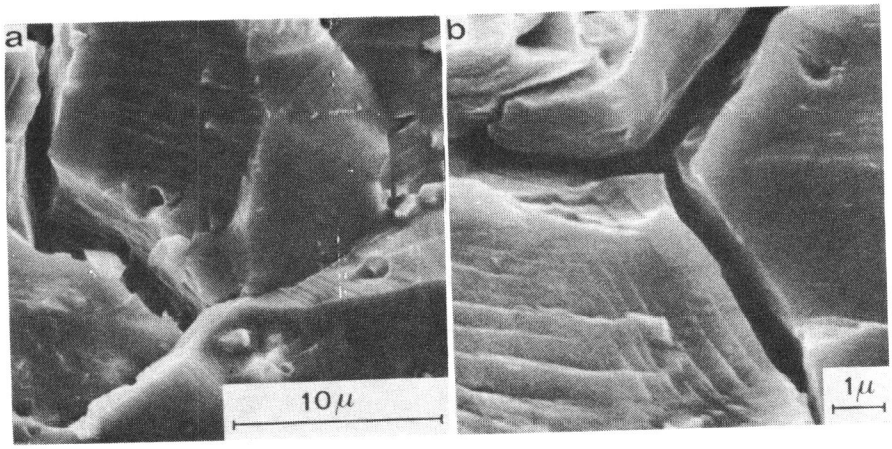

Fig. 7 SEM Fractographs Showing the Grain Surfaces Covered with Slip Lines